Geoscientific
Model Development

The DeepMIP contribution to PMIP4: experimental design for model simulations of the EECO, PETM, and pre-PETM (version 1.0)

Daniel J. Lunt[1], Matthew Huber[2], Eleni Anagnostou[9], Michiel L. J. Baatsen[3], Rodrigo Caballero[4], Rob DeConto[5], Henk A. Dijkstra[3], Yannick Donnadieu[6], David Evans[31], Ran Feng[8], Gavin L. Foster[9], Ed Gasson[5], Anna S. von der Heydt[3], Chris J. Hollis[10], Gordon N. Inglis[32], Stephen M. Jones[34], Jeff Kiehl[29], Sandy Kirtland Turner[11], Robert L. Korty[12], Reinhardt Kozdon[13], Srinath Krishnan[7], Jean-Baptiste Ladant[6], Petra Langebroek[14], Caroline H. Lear[15], Allegra N. LeGrande[16], Kate Littler[17], Paul Markwick[18], Bette Otto-Bliesner[8], Paul Pearson[15], Christopher J. Poulsen[19], Ulrich Salzmann[20], Christine Shields[8], Kathryn Snell[21], Michael Stärz[22], James Super[7], Clay Tabor[8], Jessica E. Tierney[23], Gregory J. L. Tourte[1], Aradhna Tripati[33], Garland R. Upchurch[24], Bridget S. Wade[25], Scott L. Wing[26], Arne M. E. Winguth[27], Nicky M. Wright[28], James C. Zachos[29], and Richard E. Zeebe[30]

[1]School of Geographical Sciences, University of Bristol, Bristol, UK
[2]Department of Earth, Atmospheric, and Planetary Sciences, Purdue University, West Lafayette, USA
[3]Institute for Marine and Atmospheric research Utrecht (IMAU), Utrecht University, Utrecht, Netherlands
[4]Department of Meteorology (MISU), Stockholm University, Stockholm, Sweden
[5]Department of Geosciences, University of Massachusetts, Amherst, USA
[6]Laboratoire des Sciences du Climat et de l'Environnement, CNRS/CEA, Gif-sur-Yvette, France
[7]Department of Geology and Geophysics, Yale University, New Haven, USA
[8]National Centre for Atmospheric Research, Boulder, USA
[9]Ocean and Earth Science, National Oceanography Centre Southampton, University of Southampton, Southampton, UK
[10]GNS Science, Lower Hutt, Wellington, New Zealand
[11]Department of Earth Sciences, University of California, Riverside, USA
[12]Department of Atmospheric Sciences, Texas A&M University, College Station, USA
[13]Lamont-Doherty Earth Observatory of Columbia University, Palisades, USA
[14]Uni Research Climate, Bjerknes Centre for Climate Research, Bergen, Norway
[15]School of Earth and Ocean Sciences, Cardiff University, Cardiff, UK
[16]NASA-GISS, New York, USA
[17]Camborne School of Mines, University of Exeter, Exeter, UK
[18]Getech Group plc, Leeds, UK
[19]Department of Earth and Environmental Sciences, University of Michigan, Ann Arbor, USA
[20]Department of Geography, Northumbria University, Newcastle upon Tyne, UK
[21]Department of Geological Sciences, University of Colorado, Boulder, USA
[22]Alfred Wegener Institute, Bremerhaven, Germany
[23]Department of Geosciences, University of Arizona, Tucson, USA
[24]Department of Biology, Texas State University, San Marcos, USA
[25]Department of Earth Sciences, University College London, London, UK
[26]Department of Paleobiology, Smithsonian Institution, Washington, D.C., USA
[27]Earth and Environmental Science, University of Texas, Arlington, USA
[28]School of Geosciences, University of Sydney, Sydney, Australia
[29]PBSci-Earth & Planetary Sciences Department, Institute of Marine Sciences, University of California, Santa Cruz, USA
[30]Department of Oceanography, University of Hawaii at Manoa, USA
[31]Department of Earth Sciences, University of St Andrews, St Andrews, UK

[32]School of Chemistry, University of Bristol, Bristol, UK
[33]Earth, Planetary, and Space Sciences, Atmospheric and Oceanic Sciences, Institute of the Environment and Sustainability, University of California, Los Angeles, USA
[34]School of Geography, Earth and Environmental Sciences, University of Birmingham, Birmingham, UK

Correspondence to: Daniel J. Lunt (d.j.lunt@bristol.ac.uk)

Abstract. Past warm periods provide an opportunity to evaluate climate models under extreme forcing scenarios, in particular high (> 800 ppmv) atmospheric CO_2 concentrations. Although a post hoc intercomparison of Eocene (~ 50 Ma) climate model simulations and geological data has been carried out previously, models of past high-CO_2 periods have never been evaluated in a consistent framework. Here, we present an experimental design for climate model simulations of three warm periods within the early Eocene and the latest Paleocene (the EECO, PETM, and pre-PETM). Together with the CMIP6 pre-industrial control and abrupt $4\times CO_2$ simulations, and additional sensitivity studies, these form the first phase of DeepMIP – the Deep-time Model Intercomparison Project, itself a group within the wider Paleoclimate Modelling Intercomparison Project (PMIP). The experimental design specifies and provides guidance on boundary conditions associated with palaeogeography, greenhouse gases, astronomical configuration, solar constant, land surface processes, and aerosols. Initial conditions, simulation length, and output variables are also specified. Finally, we explain how the geological data sets, which will be used to evaluate the simulations, will be developed.

1   Introduction

There is a large community of Earth scientists with strong interests in "deep-time" palaeoclimates, here defined as climates of the pre-Pliocene (i.e. prior to ~ 5 Ma). Recently, a growing community of modelling groups focussing on these periods is also beginning to emerge. DeepMIP – the Deep-time Model Intercomparison Project – brings together modellers, the data community, and other scientists into a multi-disciplinary international effort dedicated to conceiving, designing, carrying out, analysing, and disseminating an improved understanding of these time periods. It also aims to assess their relevance for our understanding of future climate change. DeepMIP is a working group in the wider Paleoclimate Modelling Intercomparison Project (PMIP4), which itself is a part of the sixth phase of the Coupled Model Intercomparison Project (CMIP6, Eyring et al., 2016). In DeepMIP, we will focus on three time periods in the latest Paleocene and early Eocene (~ 55–50 Ma), and for the first time,

carry out a formal coordinated model–data intercomparison. In addition to the experimental design presented here, DeepMIP will synthesize existing climate proxy records, and develop new ones if appropriate. The aim will be to effectively characterize our understanding of the palaeoclimate of the chosen interval through the synthesis of climate proxy records, to compare this with the model simulations, and to understand the reasons for the intra- and inter-model and data differences. The ultimate aim is to encourage model development in response to any robust model deficiencies that emerge from the model–data comparison. This is of particular relevance to models that are also used for future climate projection, given the relative warmth and high CO_2 that characterizes many intervals of deep-time.

2   Previous work

An informal, post hoc model–data intercomparison has previously been carried out for the early Eocene (Lunt et al., 2012). This compared the results of four models from five modelling groups with marine and terrestrial data syntheses, and explored the reasons for the model–model differences using energy balance diagnostics. That study contributed to the recent IPCC AR5 report (Box 5.1, Fig. 1), but it also revealed challenging differences between model simulations of this period and intriguing model–data mismatches, as well as inconsistencies between proxies (Fig. 1). For example, proxy-derived SST estimates indicate a weak meridional temperature gradient during the early Eocene which cannot easily be reconciled with the model simulations. Further work resulting from this intercomparison included that of Gasson et al. (2014), who investigated the CO_2 thresholds for Antarctic ice sheet inception; Lunt et al. (2013), who compared the ensemble and data to further Eocene simulations; and Carmichael et al. (2016), who investigated the hydrological cycle across the ensemble and compared model results with proxies for precipitation.

The previous exercise points to the need for a more coordinated experimental design (different modelling groups had carried out simulations with different boundary conditions, and different initial conditions, etc.), and a greater understanding of the reasons behind differences between different
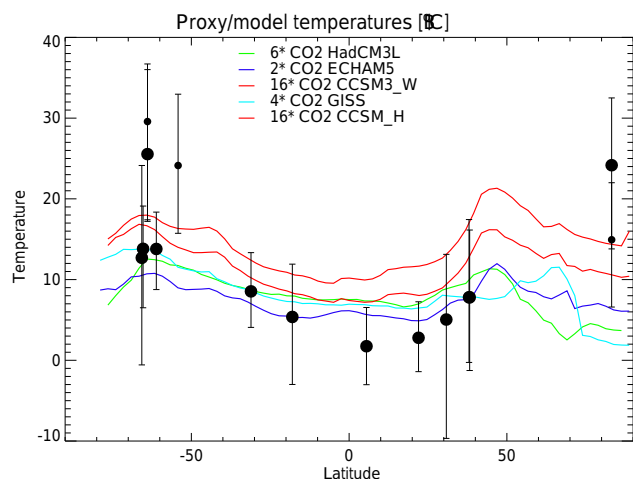
Figure 1. Zonal mean Eocene sea-surface temperature warming, presented as an anomaly relative to present or pre-industrial values. Warming from the five models in "Eomip" (Lunt et al., 2012) are shown as coloured lines; for each model only the CO_2 concentration that best fits the temperature proxy observations is shown. Warming derived from the proxies are shown as filled circles, with error bars representing the range of uncertainty associated with proxy calibration and temporal variability. Larger symbols represent "background" early Eocene state, smaller symbols represent the EECO. Adapted from Fig. 8a in Lunt et al. (2012).

climate proxies. Those challenges provide the motivation for DeepMIP.

3 The chosen intervals – the Early Eocene Climatic Optimum (EECO) the Paleocene–Eocene Thermal Maximum (PETM), and the pre-PETM.

The choice of a time interval on which to focus is based on a balance between (i) the magnitude of the anticipated climate signal (larger signals have a higher signal-to-uncertainty ratio, and larger signals provide a greater challenge to models), (ii) the uncertainties in boundary conditions that characterize the interval (small uncertainties result in more robust conclusions as to the models' abilities, and minimize the model sensitivity studies required to explore the uncertainties), and (iii) the amount and geographic distribution of palaeoclimate data available with which to evaluate the model simulations.

We have chosen to focus on the latest Paleocene and early Eocene – ~ 55 to ~ 50 Ma (the Ypresian stage), as it is the most recent geological interval characterized by high (> 800 ppmv) atmospheric CO_2 concentrations. Within the latest Paleocene and early Eocene, DeepMIP will focus on three periods (see Fig. 2):

1. The Early Eocene Climatic Optimum (EECO, ~ 53–51 Ma) which is the period of greatest sustained (> 1 Myr) warmth in the last 65 million years.

2. The Paleocene–Eocene Thermal Maximum (PETM, ~ 55 Ma) which is the event of greatest warmth in the last 65 million years.

3. The period just before the PETM (pre-PETM, or latest Paleocene) which is relatively warm compared with modern, but is cooler than both the PETM and the EECO.

These intervals have been the focus of numerous studies in the geological literature, and some syntheses of proxies from these intervals already exist (e.g. Huber and Caballero, 2011; Lunt et al., 2012; Dunkley Jones et al., 2013). The pre-PETM provides a reference point for both the PETM and the EECO. In addition, all three time periods can be referenced to modern or pre-industrial. This is in recognition that both modelling and proxies are most robust when considering relative changes, as opposed to absolutes.

Compared to earlier warm periods, such as the mid-Cretaceous, the palaeogeography during the early Eocene is reasonably well constrained, and freely available digital palaeogeographic data sets exist; however, there are wide uncertainties in estimates of atmospheric CO_2 at this time. Furthermore, due at least in part to interest in the Eocene and PETM for providing information of relevance to the future (e.g. Anagnostou et al., 2016; Zeebe et al., 2016), there is a relative wealth of climate proxy data with which the model results can be compared.

4 Experimental design

The DeepMIP experimental protocol consists of five main simulations – pre-industrial, future, two in the early Eocene (EECO and PETM), and one in the latest Paleocene (pre-PETM), plus a number of optional sensitivity studies (see Sect. 4.3). The simulations are summarized in Table 1.

4.1 Pre-industrial and future simulations

The pre-industrial simulation should be as close as possible to the CMIP6 standard, *piControl* (Eyring et al., 2016). Many groups will already have carried out this simulation as part of CMIP6. Some groups may need to make changes to their CMIP6 model configuration for the DeepMIP palaeoclimate simulations (for example changes to ocean diffusivity). If this is the case, we encourage groups to carry out a new pre-industrial simulation with the model configuration used for DeepMIP palaeoclimate simulations.

The future simulation is the CMIP6 standard *abrupt-4xCO2* simulation (Eyring et al., 2016), which branches off from the *piControl* simulation, and in which atmospheric CO_2 is abruptly quadrupled and then held constant for at least 150 years.
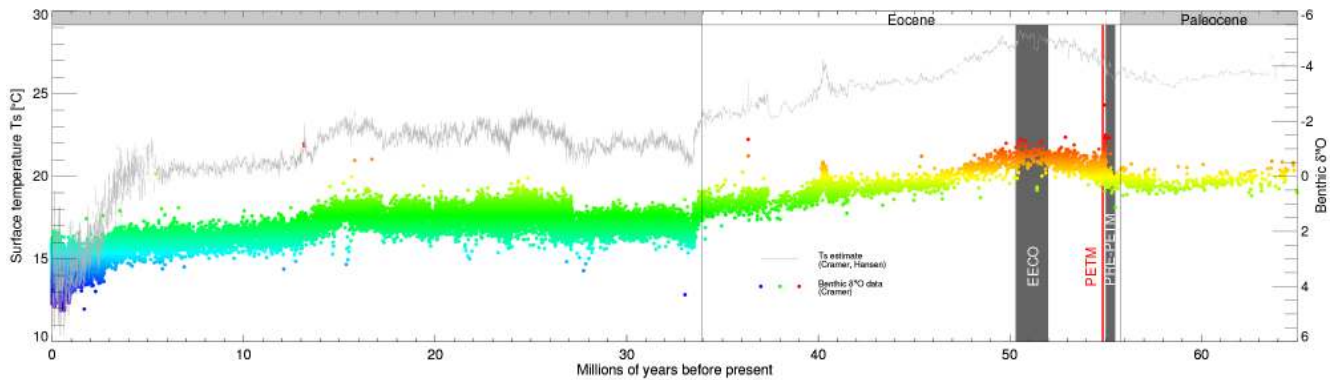
Figure 2. The three DeepMIP palaeointervals – EECO (grey shaded region), pre-PETM (grey shaded region), and the PETM (vertical red line). Also shown for context is the climate evolution over the last 65 million years, as expressed by the benthic oxygen isotope record of Cramer et al. (2009) (coloured dots), and a global annual mean surface temperature record produced by applying the methodologies of Hansen et al. (2013) to the Cramer et al. (2009) $\delta^{18}O_{benthic}$ data, and applying a 10-point running average (grey line). Note that the formal definition of the start and end date of each time period is still to be finalized.

Table 1. Summary of simulations associated with DeepMIP, including two relevant simulations from CMIP6 (*piControl* and *abrupt-4xCO2*), the three standard simulations (*deepmip-stand-X*), and some of the suggested sensitivity studies (*deepmip-sens-X*).

Simulation name	Simulation description	CO_2 [ppmv]	Palaeogeography
piControl	Pre-industrial control (Eyring et al., 2016)	280[a]	Modern
abrupt-4xCO2	Abrupt increase to $4\times CO_2$ concentrations (Eyring et al., 2016)	1120	Modern
deepmip-stand-3xCO2	Pre-PETM, at $3\times$ pre-industrial CO_2	840	Herold et al. (2014)
deepmip-stand-6xCO2	EECO/PETM, at $6\times$ pre-industrial CO_2	1680	Herold et al. (2014)
deepmip-stand-12xCO2	EECO/PETM, at $12\times$ pre-industrial CO_2	3360	Herold et al. (2014)
deepmip-sens-YxCO2	Sensitivity study at $Y\times$ pre-industrial CO_2	$Y\times 280$	Herold et al. (2014)
deepmip-sens-geoggetech	Sensitivity study with modified palaeogeography	840, 1680, 3360[b]	Lunt et al. (2016)
deepmip-sens-geogpalmag	Sensitivity study with modified palaeogeography	840, 1680, 3360[b]	This paper

[a] If a value different from 280 ppmv is used for *piControl*, then all other CO_2 values in the table should be changed accordingly. [b] Order of priority, highest priority first.

4.2 EECO/PETM and pre-PETM simulations

This section describes the DeepMIP palaeoclimate simulations. There are three standard palaeoclimate simulations (*deepmip-stand-3xCO2*, *deepmip-stand-6xCO2*, *deepmip-stand-12xCO2*), which differ only in their atmospheric CO_2 concentration, plus a number of optional sensitivity studies. In general terms, we consider the *deepmip-stand-3xCO2* simulation as representative of the pre-PETM, and the other two simulations as representing two different scenarios for the EECO and/or PETM.

4.2.1 Palaeogeography and land–sea mask

Herold et al. (2014, henceforth H14) is a peer-reviewed, traceable, freely available digital reconstruction of the early Eocene interval. It includes topography and sub-gridscale topography, bathymetry, tidal dissipation, vegetation, aerosol distributions, and river runoff. The palaeogeography from

H14 should be used for all the standard DeepMIP palaeo-climate simulations (see Table 1); they are provided digitally in netcdf format in the Supplement of H14 (see Table 2), at a resolution of $1° \times 1°$, and are illustrated here in Fig. 3a. The palaeogeographic height should be applied as an absolute, rather than as an anomaly to the pre-industrial topography. Most models additionally require some fields related to the sub-gridscale orography to be provided. Because sub-gridscale orographies are very sensitive to the resolution of the underlying data set, the sub-gridscale orography (if it is required by the model) can be estimated based on fields also provided in Supplement of H14. This can be implemented as the modelling groups see fit, but care should be taken that the pre-industrial and Eocene sub-gridscale topographies are as consistent as possible. In addition, the code used to calculate the sub-gridscale orographies in the CESM (Gent et al., 2011) model is also provided in the Supplement of H14.

Table 2. Location and filenames of the DeepMIP boundary conditions.

Simulation name(s)	Boundary condition	Location	Filename	Variable name
deepmip-stand-XxCO2[a]	Topography	Supplement of H14	herold_etal_eocene_topo_1x1.nc	topo
deepmip-stand-XxCO2	Vegetation	Supplement of H14	herold_etal_eocene_biome_1x1.nc	eocene_biome[b]
deepmip-stand-XxCO2	Runoff	Supplement of H14	herold_etal_eocene_runoff_1x1.nc	RTM_FLOW_DIRECTION
deepmip-sens-geoggetech	Topography	Supplement of Lunt et al. (2016)	bath_ypr.nc, orog_ypr.nc	bathuk, oroguk
deepmip-sens-geogpalmag	Topography	Supplement of this paper	Herold2014_TPW.nc	Band1

[a] Where *X* can be 3, 6, or 12.
[b] 27 biomes. For simplified 11 biomes, use variable eocene_biome-hp.
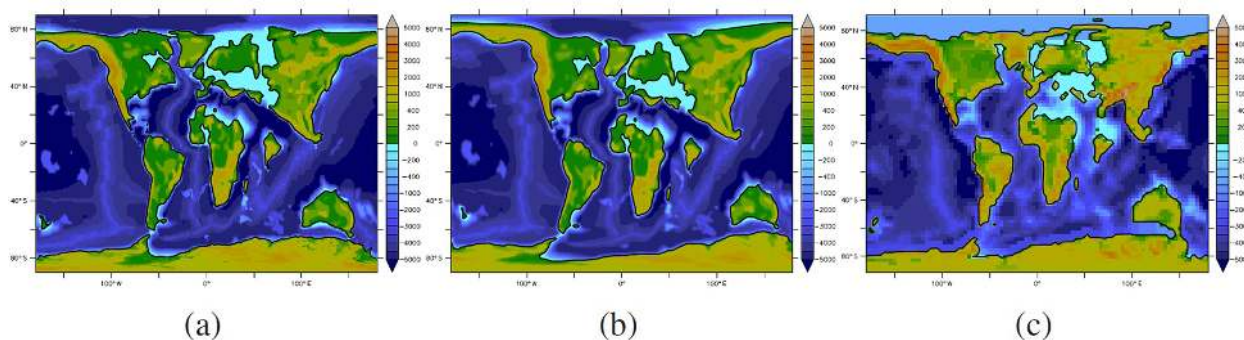

Figure 3. Orography and bathymetry for the palaeoclimate simulations in DeepMIP (metres). **(a)** The Herold et al. (2014) palaeogeography, as used in the standard palaeoclimate simulations (*deepmip-stand-3xCO2*, *deepmip-stand-6xCO2*, *deepmip-stand-9xCO2*). **(b)** The Herold et al. (2014) palaeogeography, but in the rotation framework given by Torsvik et al. (2012), which is based on a palaeomagnetic reference frame (Baatsen et al., 2016). **(c)** The Ypresian palaeogeography from Lunt et al. (2016). The location of digital versions of these three palaeogeographies is given in Table 2.

The land–sea mask can be initially calculated from the palaeogeographic height, by assigning ocean to palaeogeographic heights less than or equal to zero. Care should be taken when defining the land–sea mask for the ocean component of the model that the various seaways are preserved at the model resolution; this may require some manual manipulation of the land–sea mask.

Included in Supplement of this paper are palaeorotations such that the modern location of grid cells in the Eocene palaeogeography can be identified, as can the Eocene location of modern grid cells.

We encourage sensitivity studies to the palaeogeography – see Sect. 4.3.2.

4.2.2 Land surface

i. *Vegetation*: the vegetation in the DeepMIP palaeoclimate simulations should be prescribed as that in H14, which is included digitally as a netcdf file in the Supplement of H14 (Table 2; note that the BIOME4 vegetation should be used rather than the Sewall vegetation, and that groups may choose to base their vegetation either on the 27 biomes or the 10 megabiomes), and

shown here in Fig. 4. Groups should make a lookup table for converting the H14 Eocene data set to a format that is appropriate for their model. To aid in this process, a modern vegetation data set is also provided in the Supplement of H14, using the same plant functional types as in the H14 Eocene reconstruction; in addition, the lookup table for the CLM (Oleson et al., 2010) land model is provided as a guide in the Supplement of this paper.

ii. *Soils*: parameters associated with soils should be given constant values over the globe, with values for these parameters (e.g. albedo, water-holding capacity, etc.) given by the global mean of the group's pre-industrial simulation.

iii. *Lakes*: no lakes should be prescribed in the DeepMIP palaeoclimate simulations, unless these are predicted dynamically by the model.

iv. *River runoff*: river runoff should be taken from the H14 reconstruction, which is included digitally as a netcdf file in the Supplement of H14 (see Table 2).
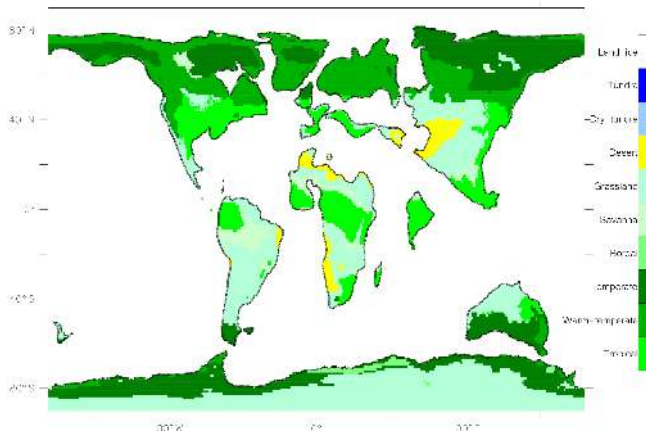
Figure 4. Vegetation, expressed as megabiomes, for the palaeoclimate simulations in DeepMIP. A netcdf file of the data at a $1° \times 1°$ resolution is available in the Supplement of Herold et al. (2014) (see Table 2).

4.2.3 Greenhouse gas concentrations

Each group should carry out three simulations at three different atmospheric CO_2 concentrations, expressed as multiples of the value in the pre-industrial simulation (typically 280 ppmv, Sect. 4.1): (i) $3\times$ pre-industrial (typically 840 ppmv), (ii) $6\times$ pre-industrial (typically 1680 ppmv), and (iii) $12\times$ pre-industrial (typically 3360 ppmv). Assuming a simple relationship between CO_2 and temperature, the benthic oxygen isotope record (see Fig. 2) implies that, within uncertainty of the CO_2 proxies, CO_2 concentrations in the EECO and PETM were similar. As such, whereas the low-CO_2 simulation can be considered as representing the pre-PETM, the two higher CO_2 simulations are intended to represent a range of possible PETM and EECO climate states. The values themselves are based primarily on recent work using boron isotopes (Anagnostou et al., 2016), which indicates that EECO CO_2 was 1625 ± 760 ppmv (Fig. 5).

It is thought that non-CO_2 greenhouse gases during the early Eocene were elevated relative to pre-industrial, especially CH_4 (e.g. ~ 3000 ppbv, Beerling et al., 2011). However, there is considerable uncertainty as to exactly how elevated they were. Given these uncertainties, and the fact that we have chosen to use a modern solar constant as opposed to a reduced solar constant (see Sect. 4.2.5), which would otherwise offset the CH_4 increase, all non-CO_2 greenhouse gases and trace gases should be set at the CMIP6 pre-industrial concentrations. In effect, we assume that the CO_2 forcing represents the CO_2, CH_4 (and other non-CO_2 greenhouse gases), and solar forcings. For reference, the radiative forcing associated with an increase in CH_4 concentrations from pre-industrial values to 3000 ppbv is $+0.98$ Wm^{-2} (Byrne and Goldblatt, 2014), and the radiative forcing associated with an decrease in solar constant from 1361 to 1355.15 Wm^{-2} (see
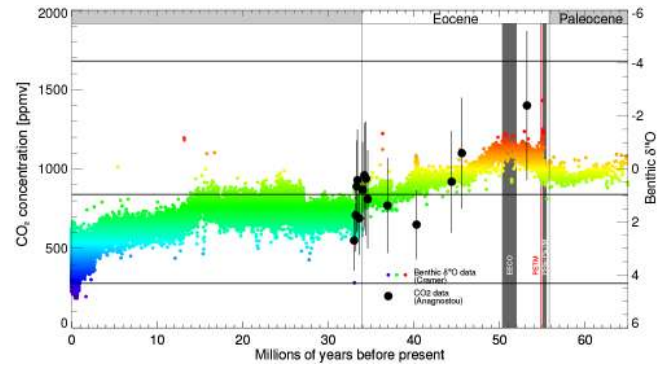

Figure 5. Atmospheric CO_2 as derived from boron isotopes in the Eocene by Anagnostou et al. (2016) (black circles and error estimates). Horizontal lines show 280 ppmv (typical pre-industrial value), and 840 and 1680 ppmv, corresponding to the *deepmip-stand-3xCO2* and *deepmip-stand-6xCO2* simulations. Also shown are the DeepMIP palaeointervals – EECO (grey shaded region), pre-PETM (grey shaded region), and the PETM (vertical red line) – and the climate evolution over the last 65 million years, as expressed by the benthic oxygen isotope record of Cramer et al. (2009) (coloured dots). Note that the formal definition of the start and end date of each time period is still to be finalized.

Sects. 4.2.5 and 4.3.5) is -1.03 Wm^{-2} (assuming a planetary albedo of 0.3).

Some groups may find the higher CO_2 simulations problematic as some models are known to develop a runaway greenhouse at high CO_2 (M. Heinemann, personal communication, 2012). In this case, in addition to the $3\times$ simulation, groups can carry out simulations at $2\times$ and $4\times$. In this way, the modelled Eocene climate sensitivity and its nonlinearities can still be investigated.

If groups only have the computational resources to carry out two simulations, they should carry out the $3\times$ and $6\times$ simulations. For groups that can only carry out a single simulation, the analysis of the runs will be limited due to the focus on anomalies in DeepMIP, but we still encourage such groups to participate; in this case they should just carry out the $3\times$ simulation.

For groups with extensive computational resources, we encourage them to carry out additional sensitivity simulations over a range of CO_2 values, and in particular at $1\times$, see Sect. 4.3.1.

4.2.4 Aerosols

The representation of aerosols (including mineral dust) in Earth system models is undergoing a period of rapid development. Therefore, we leave the implementation of aerosol fields or emissions rather flexible, and give several options. Groups may choose to (i) leave aerosol distributions or emissions identical to pre-industrial (taking account of the changed land–sea mask), or (ii) treat aerosols prognostically, or (iii) use aerosol concentrations (including mineral dust)

from H14, or (iv) use aerosol optical depths from H14, or (v) some combination of the above, depending on the aerosol type. The crucial thing is that groups are asked to document exactly how they have implemented aerosols.

4.2.5 Solar constant and astronomical parameters

All simulations should be carried out with the same solar constant and astronomical parameters as in the pre-industrial simulation. The solar constant in the CMIP6 *piControl* simulation is defined as $1361.0\,\mathrm{W\,m^{-2}}$ (Matthes et al., 2016). Although the early Eocene (51 Ma) solar constant was $\sim 0.43\,\%$ less than this (Gough, 1981), i.e. $\sim 1355\,\mathrm{W\,m^{-2}}$, we choose to use a modern value in order to (i) aid comparison of any $1\times CO_2$ simulations (see Sect. 4.3.1) with pre-industrial simulations, and (b) to offset the absence of elevated CH_4 in the experimental design (see Sect. 4.2.3). As with all of Earth history, astronomical conditions varied throughout the early Eocene. There is some evidence that the PETM and other Paleogene hyperthermals may have been paced by astronomical forcing (Lourens et al., 2005; Lunt et al., 2011), but the phase of the response relative to the forcing is unknown. The modern orbit has relatively low eccentricity, and so represents a forcing close to the long-term average, and also facilitates comparison with the control pre-industrial simulation. However, we do encourage sensitivity studies to astronomical configuration (see Sect. 4.3.3).

4.2.6 Initial conditions

i. *Atmosphere and land surface*: simulations may be initialized with any state of the atmosphere and land surface, as long as the initial condition would not typically take longer than ~ 50 years to spin up in a model with fixed sea-surface temperatures; for example, initial snow cover should not be hundreds of metres depth.

ii. *Ocean*: given that even with relatively long simulations, some vestiges of the initial ocean temperature and salinity structure will remain at the end of the simulations, we recommend that all groups adopt the same initialization procedure for the ocean, but encourage groups to carry out sensitivity studies to the initialization (see Sect. 4.3.7). The ocean should be initialized as stationary, with no initial sea ice, and a zonally symmetric temperature (T, °C) and globally constant salinity (S, psu) distribution given by the following:

$$T\,[\mathrm{°C}] = \begin{cases} \left(\frac{5000-z}{5000}25\cos(\phi)\right)+15 & \text{if } z \le 5000\,\mathrm{m} \\ 15 & \text{if } z > 5000\,\mathrm{m} \end{cases}$$
$$S\,[\mathrm{psu}] = 34.7, \tag{1}$$

where ϕ is latitude, and z is depth of the ocean (metres below surface).

Some groups have previously found that initializing the model with relatively cold ($< 10\,\mathrm{°C}$) ocean temperatures at depth results in a relatively long spinup (> 5000 years), due to the suppression of convection – hence the relatively warm initial temperatures at depth prescribed here. Groups for which the recommended initial temperature structure still results in a stratified ocean with little convection, and hence are likely to have long equilibration timescales (for example those with a model with a particularly high climate sensitivity), may wish to initialize their model with warmer deep ocean temperatures. If so, this should be clearly documented.

The value of 34.7 psu is the same as the modern mean ocean value. Although the lack of ice sheets in the Eocene would result in a decrease in mean ocean salinity relative to the modern of about 0.6 psu, on these timescales long-term geological sources and sinks of NaCl associated with crustal recycling also play an important role; Hay et al. (2006) estimate mean ocean salinity to be between 35.1 and 36.5 during the Eocene. Given the uncertainties, we choose a modern value for simplicity. If groups prefer to initialize salinity with a non-homogeneous distribution, or with a different absolute value, they may do this, but it should be documented.

For simulations in which oxygen, carbon or other isotopic systems or passive tracers are included, these can be initialized as each individual group sees fit.

4.2.7 Length of simulation

Simulations should be carried out for as long as possible. Ideally, simulations should be (a) at least 1000 years in length, and (b) have an imbalance in the top-of-atmosphere net radiation of less than $0.3\,\mathrm{W\,m^{-2}}$ (or have a similar imbalance to that of the pre-industrial control), and (c) have sea-surface temperatures that are not strongly trending (less than $0.1\,\mathrm{°C}$ per century in the global mean). Climatologies should be calculated based on the final 100 years of the simulation.

4.2.8 Output format

We strongly recommend that DeepMIP model output should be uploaded to the anticipated PMIP4 component of the CMIP6 database (Eyring et al., 2016), distributed through the Earth System Grid Federation (ESGF). However, if this is not possible, then netcdf files of the variables in Appendix A, including Tables A1–A3, should be uploaded to the Deep-MIP Model Database, which will be set up if and when required. In any case, for the "highest priority" variables in Appendix A, Tables A1–A3, all months of the simulations should be retained, such that averages can be calculated from arbitrary years of the simulation, and such that equilibrium states can be estimated using the approach of Gregory et al. (2004).

4.3 Sensitivity studies

Sections 4.1 and 4.2 give a summary of the five main simulations. Here we outline some optional sensitivity studies that groups may wish to carry out, although there is no guarantee that other groups will do the same simulations.

4.3.1 Sensitivity to CO$_2$

Groups may wish to explore more fully the sensitivity of their model to CO$_2$, and associated non-linearities (e.g. Caballero and Huber, 2013), by carrying out additional simulations over a range of CO$_2$. Normally these would be multiples of the pre-industrial concentration, in addition to the standard 3×, 6×, and 12× simulations. In particular, we encourage groups to carry out a 1× simulation, for comparison with the pre-industrial control – this simulation enables the contribution of non-CO$_2$ forcings (palaeogeography and ice sheets) to early Eocene warmth to be evaluated.

4.3.2 Sensitivity to palaeogeography

Getech Group plc (www.getech.com) have provided an alternative palaeogeographic reconstruction that may be used for sensitivity studies, in particular the simulation *deepmip-sens-geoggetech* (see Tables 1, 2). It is included digitally in Lunt et al. (2016) as a netcdf file at a resolution of 3.75° longitude × 2.5° latitude, and is shown in Fig. 3c. Because a high-resolution version of this topography is not available, groups will need to use the sub-gridscale palaeogeography from the H14 reconstruction, and interpolate to the new land–sea mask as appropriate. The vegetation, river routing, etc. from H14 will also need to be extrapolated to the new land–sea mask. Ideally, groups would carry out these simulations at the same three CO$_2$ levels as in the standard simulations, but if groups can only carry out a limited number of simulations with this palaeogeography, they should carry them out in the following order of priority (highest priority first): 3×, 6×, 12×.

Both Getech and H14 use the plate rotation model of Müller et al. (2008), which is derived from relative plate motions tied to a mantle reference frame. In their recent study, van Hinsbergen et al. (2015) argue that for palaeoclimate studies, plate motions should be tied to the spin axis of the Earth using a palaeomagnetic reference frame in order to obtain accurate estimates of palaeolatitude. For this reason, we also provide an additional version of the H14 palaeogeography, but rotated to a palaeomagnetic reference frame based on the methods outlined by van Hinsbergen et al. (2015) and Baatsen et al. (2016), for use in sensitivity study *deepmip-sens-geogpalmag* (see Tables 1, 2). This is shown in Fig. 3b, and provided in the Supplement to this paper.

Furthermore, some of the topographic features could have evolved significantly throughout the ∼ 55–51 Ma period of interest, making it unlikely that a single palaeogeography can represent all the DeepMIP time periods to the same extent.

Groups are therefore encouraged to carry out sensitivity studies around the H14 palaeogeography, to explore the uncertainties in climate which may result from uncertainties in the spatial and temporal evolution of different topographic features. These studies may include the widening or constricting and shallowing or deepening of key ocean gateways, changing the bathymetry and extent of ocean shelves, and raising or lowering mountain ranges. In particular, we encourage groups to carry out sensitivity studies in which the NE Atlantic–Arctic gateway to the east of Greenland is closed. This is because there is evidence that a short, transient period of approximately kilometre-scale tectonic uplift of NW Europe and Greenland, associated with the North Atlantic Large Igneous Province, severely restricted the NE Atlantic–Arctic oceanic gateway during the PETM period in comparison with the pre-PETM and EECO periods (Hartley et al., 2011; Jones and White, 2003; Maclennan and Jones, 2006; Saunders et al., 2007).

4.3.3 Sensitivity to astronomical parameters

Evidence of cyclicity during the Paleocene and early Eocene indicates that a component of the warmth of the PETM may be astronomically forced (Lourens et al., 2005; Westerhold et al., 2007; Galeotti et al., 2010). As such, we encourage sensitivity studies of astronomical configuration. As the standard DeepMIP palaeoclimate simulations are configured with a modern orbit, which has relatively low eccentricity, we suggest groups carry out additional simulations with high eccentricity ($e = 0.054$ compared with a modern value of $e = 0.017$), with Northern Hemispheric winter corresponding with both aphelion and perihelion.

4.3.4 Sensitivity to vegetation

Those groups which have a model that includes dynamic vegetation may carry out sensitivity studies with dynamic vegetation turned on. The initial condition should be broadleaf or needleleaf trees at all locations. Ideally groups would carry out these simulations at the same three CO$_2$ levels as in the standard simulations, but if groups can only carry out a limited number of simulations with the dynamic vegetation, they should carry them out in the following order of priority (highest priority first): 3×, 6×, 12×. Groups with models that include a dynamic vegetation component can choose to pass to their vegetation model either the ambient atmospheric CO$_2$ or a lower concentration if required for model stability.

4.3.5 Sensitivity to solar constant

Groups may wish to explore the relative radiative forcing of the solar luminosity compared with other forcings, by carrying out an Eocene simulation with a reduced solar luminosity. The suggested reduction is 0.43 % (Gough, 1981), which would normally be from 1361.0 W m^{-2} in the mod-

ern to $1355.15\,\mathrm{W\,m^{-2}}$ in the Eocene. This would typically be carried out at a CO_2 level of $3\times$.

4.3.6 Sensitivity to non-CO_2 greenhouse gases

Groups may choose to explore sensitivity to non-CO_2 greenhouse gases (see Sect. 4.2.3 for discussion of CH_4), in particular if these can be predicted by the model interactively.

4.3.7 Sensitivity to initialization

We encourage groups to carry out sensitivity studies to the initialization of the ocean temperature and salinity. It is possible that models will exhibit bistability with respect to initial condition, and as discussed in Sect. 4.2.6 we expect that the equilibration time will be a function of the initial conditions and will be different for different models.

4.3.8 "Best in show"

Participants are invited to carry out simulations in which they attempt to best-match existing climate proxy data. This may be done in a number of ways, for example by modifying the aerosols (Huber and Caballero, 2011), cloud properties (Kiehl and Shields, 2013), physics parameters (Sagoo et al., 2013), using very high CO_2 (Huber and Caballero, 2011), incorporating dynamic vegetation (Loptson et al., 2014), modifying gateways (Roberts et al., 2009), modifying orbital configuration, including non-CO_2 greenhouse gases, or a combination of the above and other modifications.

5 Climate proxies

A major focus of DeepMIP will be to develop a new synthesis of climate proxy data for the latest Paleocene and early Eocene, focussing on the three targeted time intervals: pre-PETM, PETM, and EECO. The main focus of DeepMIP will be on temperature and precipitation proxies. Two working groups have been set up to compile these data from marine and terrestrial records. These groups will also work together to generate new data sets for poorly documented regions, such as the tropics, and will seek multiple lines of evidence for climate reconstructions wherever possible. The marine working group is excited by the possibility of using innovative analytical techniques (e.g. Kozdon et al., 2013) to recover robust estimates for sea-surface temperature from planktic foraminiferal assemblages within legacy sediment cores of the International Ocean Discovery Program. Published data sets will be combined into an open-access online database. The EECO and PETM or pre-PETM marine compilations of Lunt et al. (2012), Hollis et al. (2012), and Dunkley Jones et al. (2013), and EECO terrestrial compilations of Huber and Caballero (2011) provide a starting point for this database. One of the great challenges for these working groups will be to develop new ways to assess climate proxy reliability and quantify uncertainties. In some cases, it may be more straightforward to consider relative changes in proxies rather than report absolute values. Climate proxy system modelling (Evans et al., 2013) coupled with Bayesian analysis (e.g. Khider et al., 2015; Tierney and Tingley, 2014) has great potential for improving estimation of uncertainties and directly linking our climate proxy compilation with the climate simulations. In addition to these quantitative estimates of uncertainty, all data will be qualitatively assessed based on expert opinion, for example by characterizing proxies as high, medium, or low confidence (as has been done in PlioMIP, see Dowsett et al., 2012).

We anticipate a companion paper to this one in which we will give more details of the DeepMIP data and associated protocols.

6 Products

In addition to this experimental design paper, and papers describing the new climate proxy syntheses, once the model simulations are complete we anticipate the production of overarching papers describing the "large-scale features" of the model simulations, and model–data comparisons. Following this, we anticipate a number of spin-off papers looking at various other aspects of the model simulations (e.g. ENSO, ocean circulation, monsoons). In particular we expect papers that explore the relevance of the DeepMIP simulations and climate proxy syntheses for future climate, for example through model developments that arise as a result of the model–data comparison, or emergent constraints (Bracegirdle and Stephenson, 2013) on global-scale metrics such as climate sensitivity. Furthermore, we will encourage modelling participants to publish individual papers that describe their own simulations in detail, including how the boundary conditions were implemented. In this respect, we are basing our dissemination strategy on that of PlioMIP (Haywood et al., 2013); see their Special Issue at http://www.geosci-model-dev.net/special_issue5.html.

7 Data availability

The boundary conditions for the standard DeepMIP palaeoclimate simulations are supplied in the Supplement of H14 (Herold et al., 2014); see Table 2. For availability of boundary conditions for DeepMIP sensitivity studies, also see Table 2. Data held in both the CMIP6 and DeepMIP Model databases, when these are operational, will likely be freely accessible through data portals after registration.

Appendix A: Output variables

As stated in Sect. 4.2.8, we strongly recommend that model output is uploaded to the CMIP6 database. If the CMIP6 database cannot be used, the variables in Tables A1–A3 should be submitted to the DeepMIP Model Database, which will be set up if and when required. Climatological averages of the final 100 years of the simulation should be supplied for each month (12 fields for each variable). In addition, for the highest priority variables, all months of the simulation should be supplied.

Furthermore, as many groups are interested in hydrological extremes, groups should aim to produce 10 years of hourly precipitation, evaporation, and runoff data.

Table A1. Atmosphere variables.

Variable	Units	Highest priority
Near-surface (1.5 m) air temperature	°C	X
Surface skin temperature	°C	
Precipitation	$kg\,m^2\,s^{-1}$	X
Total evaporation	$kg\,m^2\,s^{-1}$	
Total cloud cover	[0, 1]	
FLNS	$W\,m^{-2}$	
FLNT	$W\,m^{-2}$	X
FSDS	$W\,m^{-2}$	
FSNS	$W\,m^{-2}$	
FSNT	$W\,m^{-2}$	X
FSDT	$W\,m^{-2}$	
Sensible heat flux	$W\,m^{-2}$	
Latent heat flux	$W\,m^{-2}$	
Near-surface (10 m) u wind	$m\,s^{-1}$	
Near-surface (10 m) v wind	$m\,s^{-1}$	
Surface wind stress (x)	$N\,m^{-2}$	
Surface wind stress (y)	$N\,m^{-2}$	
Mean sea-level pressure	Pa	
Surface pressure	Pa	
u winds on model atmospheric levels	$m\,s^{-1}$	
v winds on model atmospheric levels	$m\,s^{-1}$	
w winds on model atmospheric levels	$m\,s^{-1}$	
u wind at 200 mbar	$m\,s^{-1}$	
v wind at 200 mbar	$m\,s^{-1}$	
u wind at 500 mbar	$m\,s^{-1}$	
v wind at 500 mbar	$m\,s^{-1}$	
u wind at 850 mbar	$m\,s^{-1}$	
v wind at 850 mbar	$m\,s^{-1}$	
Geopotential height at 200 mbar	m	
Geopotential height at 500 mbar	m	
Geopotential height at 850 mbar	m	
Temperature at 200 mbar	°C	
Temperature at 500 mbar	°C	
Temperature at 850 mbar	°C	
Specific humidity at 200 mbar	$kg\,kg^{-1}$	
Specific humidity at 500 mbar	$kg\,kg^{-1}$	
Specific humidity at 850 mbar	$kg\,kg^{-1}$	

N.B. *Fxyz* notation
F = flux
x = S(hortwave) or L(ongwave)
y = D(own) or N(et)
z = S(urface) or T(op of atmosphere)

Table A2. Ocean variables.

Variable	Units	Highest priority
Sea-surface temperature	°C	X
Sea-ice fraction	[0, 1]	X
u, v, w on model levels	$\mathrm{cm\,s^{-1}}$	
Potential temperature on model levels	°C	
Salinity on model levels	psu	
Barotropic streamfunction	$\mathrm{cm^3\,s^{-1}}$	
Mixed-layer depth	m	
Global overturning streamfunction	Sv	

Table A3. Boundary conditions.

Variable	Units
Land–sea mask	[0, 1]
Topography	m
Bathymetry	m

References

Anagnostou, E., John, E., Edgar, K., Foster, G., Ridgwell, A., Inglis, G., Pancost, R., Lunt, D., and Pearson, P.: Changing atmospheric CO_2 concentration was the primary driver of early Cenozoic climate, Nature, 533, 380–384, doi:10.1038/nature17423, 2016.

Baatsen, M., van Hinsbergen, D. J. J., von der Heydt, A. S., Dijkstra, H. A., Sluijs, A., Abels, H. A., and Bijl, P. K.: Reconstructing geographical boundary conditions for palaeoclimate modelling during the Cenozoic, Clim. Past, 12, 1635–1644, doi:10.5194/cp-12-1635-2016, 2016.

Beerling, D. J., Fox, A., Stevenson, D. S., and Valdes, P. J.: Enhanced chemistry-climate feedbacks in past greenhouse worlds, P. Natl. Acad. Sci. USA, 108, 9770–9775, 2011.

Bracegirdle, T. J. and Stephenson, D. B.: On the Robustness of Emergent Constraints Used in Multimodel Climate Change Projections of Arctic Warming, J. Climate, 26, 669–678, 2013.

Byrne, B. and Goldblatt, C.: Radiative forcing at high concentrations of well-mixed greenhouse gases, Geophys. Res. Lett., 41, 152–160, 2014.

Caballero, R. and Huber, M.: State-dependent climate sensitivity in past warm climates and its implications for future climate projections, P. Natl. Acad. Sci. USA, 110, 14162–14167, 2013.

Carmichael, M. J., Lunt, D. J., Huber, M., Heinemann, M., Kiehl, J., LeGrande, A., Loptson, C. A., Roberts, C. D., Sagoo, N., Shields, C., Valdes, P. J., Winguth, A., Winguth, C., and Pancost, R. D.: A model–model and data–model comparison for the early Eocene hydrological cycle, Clim. Past, 12, 455–481, doi:10.5194/cp-12-455-2016, 2016.

Cramer, B. S., Toggweiler, J. R., Wright, J. D., Katz, M. E., and Miller, K. G.: Ocean overturning since the Late Cretaceous: Inferences from a new benthic foraminiferal isotope compilation, Paleoceanography, 24, PA4216, doi:10.1029/2008PA001683, 2009.

Dowsett, H. J., Robinson, M. M., Haywood, A. M., Hill, D. J., Dolan, A. M., Stoll, D. K., Chan, W.-L., Abe-Ouchi, A., Chandler, M. A., Rosenbloom, N. A., Otto-Bliesner, B. L., Bragg, F. J., Lunt, D. J., Foley, K. M., and Riesselman, C. R.: Assessing confidence in Pliocene sea surface temperatures to evaluate predictive models, Nature Climate Change, 2, 365–371, 2012.

Dunkley Jones, T., Lunt, D., Schmidt, D., Ridgwell, A., Sluijs, A., Valdes, P., and Maslin, M.: Climate model and proxy data constraints on ocean warming across the Paleocene-Eocene Thermal Maximum, Earth-Sci. Rev., 125, 123–145, doi:10.1016/j.earscirev.2013.07.004, 2013.

Evans, M. N., Tolwinski-Ward, S. E., Thompson, D. M., and Anchukaitis, K. J.: Applications of proxy system modeling in high resolution paleoclimatology, Quaternary Sci. Rev., 76, 16–28, 2013.

Eyring, V., Bony, S., Meehl, G. A., Senior, C. A., Stevens, B., Stouffer, R. J., and Taylor, K. E.: Overview of the Coupled Model Intercomparison Project Phase 6 (CMIP6) experimental design and organization, Geosci. Model Dev., 9, 1937–1958, doi:10.5194/gmd-9-1937-2016, 2016.

Galeotti, S., Krishnan, S., Pagani, M., Lanci, L., Gaudio, A., Zachos, J. C., Monechi, S., Morelli, G., and Lourens, L.: Orbital chronology of Early Eocene hyperthermals from the Contessa Road section, central Italy, Earth Planet. Sc. Lett., 290, 192–200, 2010.

Gasson, E., Lunt, D. J., DeConto, R., Goldner, A., Heinemann, M., Huber, M., LeGrande, A. N., Pollard, D., Sagoo, N., Siddall, M., Winguth, A., and Valdes, P. J.: Uncertainties in the modelled CO_2 threshold for Antarctic glaciation, Clim. Past, 10, 451–466, doi:10.5194/cp-10-451-2014, 2014.

Gent, P., Danabasoglu, G., Donner, L., Holland, M., Hunke, E., Jayne, S., Lawrence, D., Neale, R., Rasch, P., Vertenstein, M., Worley, P., Yang, Z.-L., and Zhang, M.: The Community Climate System Model Version 4, J. Climate, 24, 49734991, doi:10.1175/2011JCLI4083.1, 2011.

Gough, D.: Solar interior structure and luminosity variations, Sol, Phys., 74, 21–34, 1981.

Gregory, J. M., W. J. Ingram, W. J., Palmer, M. A., Jones, G. S., Stott, P. A., Thorpe, R. B., Lowe, J. A., Johns, T. C., and Williams, K. D.: A new method for diagnosing radiative forcing and climate sensitivit, Geophys. Res. Lett., 31, L03205, doi:10.1029/2003gl018747, 2004.

Hansen, J., Sato, M., Russell, G., and Kharecha, P.: Climate sensitivity, sea level and atmospheric carbon dioxide, Philos. T. Roy. Soc. A, 371, 20120294, doi:10.1098/rsta.2012.0294, 2013.

Hartley, R. A., Roberts, G., White, N., and Richardson, C. J.: Transient convective uplift of an ancient buried landscape, Nat. Geosci., 4, 562–565, 2011.

Hay, W. W., Migdisov, A., Balukhovsky, A. N., Wold, C. N., Flögel, S., and Söding, A.: Evaporites and the salinity of the ocean during the Phanerozoic: Implications for climate, ocean circulation and life, Palaeogeogr. Palaeocl., 240, 3–46, 2006.

Haywood, A. M., Hill, D. J., Dolan, A. M., Otto-Bliesner, B. L., Bragg, F., Chan, W.-L., Chandler, M. A., Contoux, C., Dowsett,

H. J., Jost, A., Kamae, Y., Lohmann, G., Lunt, D. J., Abe-Ouchi, A., Pickering, S. J., Ramstein, G., Rosenbloom, N. A., Salzmann, U., Sohl, L., Stepanek, C., Ueda, H., Yan, Q., and Zhang, Z.: Large-scale features of Pliocene climate: results from the Pliocene Model Intercomparison Project, Clim. Past, 9, 191–209, doi:10.5194/cp-9-191-2013, 2013.

Herold, N., Buzan, J., Seton, M., Goldner, A., Green, J. A. M., Müller, R. D., Markwick, P., and Huber, M.: A suite of early Eocene (~ 55 Ma) climate model boundary conditions, Geosci. Model Dev., 7, 2077–2090, doi:10.5194/gmd-7-2077-2014, 2014.

Hollis, C. J., Taylor, K. W. T., Handley, L., Pancost, R. D., Huber, M., Creech, J., Hines, B., Crouch, E. M., Morgans, H. E. G., Crampton, J. S., Gibbs, S., Pearson, P., and Zachos, J. C.: Early Paleogene temperature history of the Southwest Pacific Ocean: reconciling proxies and models, Earth Planet. Sc. Lett., 349-350, 53–66, 2012.

Huber, M. and Caballero, R.: The early Eocene equable climate problem revisited, Clim. Past, 7, 603–633, doi:10.5194/cp-7-603-2011, 2011.

Jones, S. M. and White, N. J.: Shape and size of the initiating Iceland Plume swell, Earth Planet. Sc. Lett., 216, 271–282, 2003.

Khider, D., Huerta, G., Jackson, C., Stott, L. D., and Emile-Geay, J.: A Bayesian, multivariate calibration for Globigerinoides ruber Mg/Ca, Geochem. Geophy. Geosy., 16, 2916–2932, doi:10.1002/2015GC005844, 2015.

Kiehl, J. T. and Shields, C. A.: Sensitivity of the Palaeocene–Eocene Thermal Maximum climate to cloud properties, Philos. T. Roy. Soc. A, 371, 20130093, doi:10.1098/rsta.2013.0093, 2013.

Kozdon, R., Kelly, D. C., Kitajima, K., Strickland, A., Fournelle, J. H., and Valley, J. W.: In situ δ^{18}O and Mg/Ca analyses of diagenetic and planktic foraminiferal calcite preserved in a deep-sea record of the Paleocene-Eocene Thermal Maximum, Paleoceanography, 28, 517–528, doi:10.1002/palo.20048, 2013.

Loptson, C. A., Lunt, D. J., and Francis, J. E.: Investigating vegetation–climate feedbacks during the early Eocene, Clim. Past, 10, 419–436, doi:10.5194/cp-10-419-2014, 2014.

Lourens, L. J., Sluijs, A., Kroon, D., Zachos, J. C., Thomas, E., Rohl, U., Bowles, J., and Raffi, I.: Astronomical pacing of late Palaeocene to early Eocene global warming events, Nature, 435, 1083–1087, 2005.

Lunt, D. J., Ridgwell, A., Sluijs, A., Zachos, J., Hunter, S., and Haywood, A.: A model for orbital pacing of methane hydrate destabilization during the Palaeogene, Nat. Geosci., 4, 775–778, 2011.

Lunt, D. J., Dunkley Jones, T., Heinemann, M., Huber, M., LeGrande, A., Winguth, A., Loptson, C., Marotzke, J., Roberts, C. D., Tindall, J., Valdes, P., and Winguth, C.: A model–data comparison for a multi-model ensemble of early Eocene atmosphere–ocean simulations: EoMIP, Clim. Past, 8, 1717–1736, doi:10.5194/cp-8-1717-2012, 2012.

Lunt, D. J., Elderfield, H., Pancost, R., Ridgwell, A., Foster, G. L., Haywood, A., Kiehl, J., Sagoo, N., Shields, C., Stone, E. J., and Valdes, P.: Warm climates of the past – a lesson for the future?, Philos. T. Roy. Soc. A, 371, 20130146, doi:10.1098/rsta.2013.0146, 2013.

Lunt, D. J., Farnsworth, A., Loptson, C., Foster, G. L., Markwick, P., O'Brien, C. L., Pancost, R. D., Robinson, S. A., and Wrobel, N.: Palaeogeographic controls on climate and proxy interpretation, Clim. Past, 12, 1181–1198, doi:10.5194/cp-12-1181-2016, 2016.

Maclennan, J. and Jones, S. M.: Regional uplift, gas hydrate dissociation and the origins of the Paleocene-Eocene Thermal Maximum, Earth Planet. Sc. Lett., 245, 65–80, 2006.

Matthes, K., Funke, B., Anderson, M. E., Barnard, L., Beer, J., Charbonneau, P., Clilverd, M. A., Dudok de Wit, T., Haberreiter, M., Hendry, A., Jackman, C. H., Kretschmar, M., Kruschke, T., Kunze, M., Langematz, U., Marsh, D. R., Maycock, A., Misios, S., Rodger, C. J., Scaife, A. A., Seppälä, A., Shangguan, M., Sinnhuber, M., Tourpali, K., Usoskin, I., van de Kamp, M., Verronen, P. T., and Versick, S.: Solar Forcing for CMIP6 (v3.1), Geosci. Model Dev. Discuss., doi:10.5194/gmd-2016-91, in review, 2016.

Müller, R. D., Sdrolias, M., Gaina, C., and Roest, W. R.: Age, spreading rates, and spreading asymmetry of the world's ocean crust, Geochem. Geophy. Geosy., 9, Q04006, doi:10.1029/2007GC001743, 2008.

Oleson, K., Lawrence, D., Bonan, G., Flanner, M., Kluzek, E., Lawrence, P., Levis, S., Swenson, S., Thornton, P., Dai, A., Decker, M., Dickinson, R., Feddema, J., Heald, C., Hoffman, F., Lamarque, J.-F., Mahowald, N., Niu, G.-Y., Qian, T., Randerson, J., Running, S., Sakaguchi, K., Slater, A., Stockli, R., Wang, A., Yang, Z.-L., Zeng, X., and Zeng, X.: Technical Description of version 4.0 of the Community Land Model (CLM), National Center for Atmospheric Research (NCAR), NCAR Technical Note NCAR/TN-478+STR, 257 pp, 2010.

Roberts, C. D., LeGrande, A. N., and Tripati, A. K.: Climate sensitivity to Arctic seaway restriction during the early Paleogene, Earth Planet. Sci. Lett., 286, 576–585, 2009.

Sagoo, N., Valdes, P., Flecker, R., and Gregoire, L.: The Early Eocene equable climate problem: can perturbations of climate model parameters identify possible solutions?, Philos. T. Roy. Soc. A, 371, 20130123, doi:10.1098/rsta.2013.0123, 2013.

Saunders, A. D., Jones, S. M., Morgan, L. A., Pierce, K. L., Widdowson, M., and Xu, Y.: The role of mantle plumes in the formation of continental large igneous provinces: Field evidence used to constrain the effects of regional uplift, Chem. Geol., 241, 282–318, 2007.

Tierney, J. E. and Tingley, M. P.: A Bayesian, spatially-varying calibration model for the TEX$_{86}$ proxy, Geochim. Cosmochim. Ac., 127, 83–106, doi:10.1016/j.gca.2013.11.026, 2014.

Torsvik, T. H., Van der Voo, R., Preeden, U., Niocaill, C. M., Steinberger, B., Doubrovine, P. V., van Hinsbergen, D. J. J., Domeier, M., Gaina, C., Tohver, E., Meert, J. G., McCausland, P. J. A., and Cocks, L. R. M.: Phanerozoic polar wander, palaeogeography and dynamics, Earth-Sci. Rev., 114, 325–368, doi:10.1016/j.earscirev.2012.06.002, 2012.

van Hinsbergen, D. J. J., de Groot, L. V., van Schaik, S. J., Spakman, W., Bijl, P. K., Sluijs, A., Langereis, C. G., and Brinkhuis, H.: A Paleolatitude Calculator for Paleoclimate Studies, PLoS ONE, 10, e0126946, doi:10.1371/journal.pone.0126946, 2015.

Westerhold, T., Rohl, U., Laskar, J., Raffi, I., Bowles, J., Lourens, L. J., and Zachos, J. C.: On the duration of magnetochrons C24r and C25n and the timing of early Eocene global warming events: Implications from the Ocean Drilling Program Leg 208 Walvis Ridge depth transect, Paleoceanography, 22, PA2201, doi:10.1029/2006PA001322, 2007.

Zeebe, R. E., Ridgwell, A., and Zachos, J. C.: Anthropogenic carbon release rate unprecedented during the past 66 million years, Nat. Geosci., 9, 325–329, 2016.